Lattice study of 3D compact QED at finite temperature

M. N. Chernodub*
ITEP, B. Cheremushkinskaya 25, Moscow, 117259, Russia

E.-M. Ilgenfritz†
Institut für Theoretische Physik, Universität Tübingen, D-72076 Tübingen, Germany

A. Schiller‡
Institut für Theoretische Physik and NTZ, Universität Leipzig, D-04109 Leipzig, Germany
(Received 5 June 2001; published 10 August 2001)

We study the deconfinement phase transition and monopole properties in a finite temperature three-dimensional compact Abelian gauge model on the lattice. We predict the critical coupling as a function of the lattice size in a simplified model to describe monopole binding. We demonstrate numerically that monopoles are sensitive to the transition. In the deconfinement phase the monopoles appear in the form of a dilute gas of magnetic dipoles. In the confinement phase both monopole density and string tension differ from semiclassical estimates if monopole binding is neglected. However, an analysis of the monopole clusters shows that the relation between the string tension and the density of monopoles in charged clusters is in reasonable agreement with predictions. We study the cluster structure of the vacuum in both phases of the model.

DOI: 10.1103/PhysRevD.64.054507 PACS number(s): 11.15.Ha, 11.10.Wx

I. INTRODUCTION

Compact Abelian gauge theory in three Euclidean dimensions is a case where permanent confinement is proven and qualitatively understood [1,2]. In order to gain some experience for more realistic theories, it is interesting to study how this mechanism ceases to work under special conditions. High temperature is such a case. In this paper we reexamine the finite temperature deconfining phase transition. We will emphasize the aspect of monopole binding which explains the breakdown of confinement. In a companion paper, we extend these studies to the case of nonvanishing external fields.

Compact QED theory possesses Abelian monopoles as topological defects appearing due to the compactness of the gauge group. Considering the three-dimensional (3D) theory as the static limit of a 4D theory, the monopoles are just *magnetic* monopoles at rest, and the components of field strength are *magnetic*. In a three-dimensional theory, the monopoles are instanton-like objects: instead of tracing world lines (as they do in four-dimensions) they occupy points. The plasma of monopoles and antimonopoles can explain the permanent confinement of oppositely charged electric test charges [1] in bound states, kept together by a linear potential. In the language of magnetostatics, confinement appears due to a screening of the magnetic field induced by the electric current circulating along the Wilson loop. Monopoles and antimonopoles form a polarized sheet of finite thickness (the ''string'') along the minimal surface spanned by the Wilson loop. The formation of the string (observed in the lattice simulations in Ref. [3]) leads, for nonvanishing electric current, to an excess of the free energy proportional to the area.

At finite temperature the phase structure becomes nontrivial. What we have in mind, is compactifying $3\mathrm{D}\rightarrow(2+1)\mathrm{D}$ in the ''temporal'' (third or z) direction. The confinement-deconfinement phase transition was studied on the lattice both analytically [4] and numerically [7]. According to Svetitsky-Yaffe universality arguments [5], an interpretation of the transition was attempted in terms of the $U(1)$ vortex dynamics of the corresponding 2D spin system. The phase transition—which is expected to be of Kosterlitz-Thouless type [6]—was demonstrated to be accompanied by restructuring of the vortex system [7]. The vortices are described by a 2D $U(1)$ spin model representing the dynamics of the Polyakov loop (also see the discussion in Ref. [4]). Approaching the transition temperature, vortices and antivortices start to form bound states. In the high temperature phase no unbound vortices and antivortices are left.

In the present paper we discuss an interpretation of deconfinement starting from the confinement picture outlined above, in terms of magnetic monopoles. The confining plasma of the monopoles and antimonopoles turns into a dipole plasma at the deconfinement phase transition. A dipole plasma is inefficient to completely screen the field created by electric currents running along the pair of Polyakov loops. In this case the screening mass vanishes while the magnetic susceptibility of the medium is smaller than unity. Both monopole and vortex binding mechanisms of the deconfinement phase transition were discussed for 3D finite temperature Georgi-Glashow model in Refs. [8] and [9], respectively.

In the finite temperature case, strictly speaking, there is a problem with calling all the fields ''magnetic,'' as we did above when we summarized the zero temperature case. Similar to Ref. [7], the confinement aspect itself will be illuminated in terms of the $U(1)$ valued Polyakov loops in the

*Email address: maxim@heron.itep.ru
†Email address: ilgenfri@alpha1.tphys.physik.uni-tuebingen.de
‡Email address: schiller@itp.uni-leipzig.de

third direction, and in terms of Polyakov loop correlators representing pairs of charges separated in 2D space. In $(2+1)$D there is no longer symmetry between the three components of the field strength tensor. The closest relative of the true magnetic field is F_{12} distinct from the others, while there is still a symmetry between F_{13} and F_{23}. With this distinction in mind one can conditionally call these ''magnetic'' and ''electric'' components of the field strength tensor, respectively. As long as one does not introduce external fields, even at finite temperature there is no need to distinguish between them. The sources of the respective fluxes will be simply called monopoles or ''magnetic charges'' in the following.

The binding of the monopoles is not isotropic. It occurs mainly in the 2D space direction due to the logarithmic potential between the monopoles separated by a large spatial distance. As a consequence of periodic boundary conditions in the temporal direction, the force between the monopoles and antimonopoles vanishes at half of the temporal extent. Therefore, the potential in the temporal direction is weaker than in the spatial directions. As a consequence, the spatial size of the monopole bound state is expected to be smaller than the size in the temporal direction. This means that the dipoles are dominantly oriented parallel or antiparallel to the third direction. The monopole deconfinement scenario raises the question of whether monopole properties (such as pairing and orientation) could be influenced by an eventual external field. This aspect will be addressed in a companion paper.

With or without an external field, the deconfining mechanism by monopole pairing seems to have interesting counterparts in more realistic gauge theories. The formation of monopole pairs is qualitatively similar to the binding of instantons in instanton molecules with increasing temperature in QCD suggested to be responsible for chiral symmetry restoration [10]. In the electroweak theory, the formation of Nambu monopole-antimonopole pairs, a remnant from a dense medium of disordered Z vortices and Nambu monopoles which characterizes the high-temperature phase, acccompanies the transition toward a low-temperature phase [11]. Also note, that a dipole vacuum, although not confining, still has a nonperturbative nature [12].

The plan of this paper is as follows. In Sec. II we estimate the critical coupling of the confinement-deconfinement phase transition based on a monopole binding model for a finite lattice. In Sec. III the transition is numerically located for a lattice size of $32^2\times 8$, and confinement properties are studied. We present various monopole properties including dipole formation based on a cluster analysis, in Sec. IV. We study the relation of the monopoles and dipoles to the phase transition in Sec. V. We briefly summarize our results Sec. VI.

II. SOME HEURISTIC CONSIDERATIONS

In 3D compact electrodynamics there are monopoles interacting via the Coulomb potentials,

$$S=\frac{g_m^2}{2}\sum_{a,b} q_a q_b V_T(\vec{x}_a-\vec{x}_b), \tag{2.1}$$

where q_a and $\vec{x}_a$ are, respectively, the charge (in units of the elementary monopole charge, $g_m=2\pi/g_3$, where g_3 is the three dimensional coupling constant) and the 3D position vector of the ath monopole. The subscript T indicates that the interaction potential V_T eventually depends on the temperature.

At zero temperature the monopoles are randomly located in Euclidean $\mathcal{R}^3$ space, and the classical interaction potential between the monopole and antimonopole is inversely proportional to the distance R between the objects, $V_0(R)=-(4\pi R)^{-1}$. At finite temperature T the monopoles live in the $\mathcal{R}^2\times\mathcal{S}_1$ space (with $\mathcal{S}_1$ being a circle of perimeter T^{-1}) and the interaction potential is modified. At small separations between the monopole and antimonopole the interaction is zero temperature like, $V_T(\mathbf{x},z)=V_0(\sqrt{\mathbf{x}^2+z^2})+\cdots$, where $\vec{x}=(x,y,z)=(\mathbf{x},z)$. At large spatial separations $\mathbf{x}$ the potential between monopoles is essentially two dimensional [8],

$$V_T(\mathbf{x},z)=-2\,T\ln|\mathbf{x}|+\cdots, \quad |\mathbf{x}|T\gg 1. \tag{2.2}$$

However, the interaction between monopoles separated by a distance z in the third (temperature) direction is of 3D Coulomb type for small spatial intermonopole distances, $|\mathbf{x}|T\ll 1$: $V_T(\mathbf{x},z)=-(4\pi z)^{-1}$, $zT\ll 1$. The force between monopoles and antimonopoles at a distance $z=1/(2T)$ vanishes due to periodicity in the temperature direction. Thus one might expect that at finite temperature the monopoles form magnetically neutral states which are bounded in spatial directions. However, the dynamics of the monopoles in the temperature direction is not restricted by a logarithmic potential.

Thus at zero temperature the system exists in the form of a Coulomb gas of magnetic monopoles and antimonopoles. In this phase the medium confines electric charges [1]. As the temperature increases, the three-dimensional Coulombic potential turns into a two-dimensional logarithmic potential for spatial monopole interactions. The monopoles and antimonopoles become weakly confined, and form more and more dipole bound states. The dipoles have a finite average spatial size (the distance between the magnetically oppositely charged constituents) which is a decreasing function of the temperature since the interaction potential between the particles rises as temperature increases; cf. Eq. (2.2).

In the low temperature regime, this dipole size would still be larger than the average distance between the particles inside the plasma, and therefore only a small fraction of monopoles residing in actual dipoles is mixed with a weakly correlated monopole-antimonopole component. At sufficiently large temperature, however, the typical dipole size becomes smaller than the interparticle distance in the plasma and the system turns into a pure dipole plasma. The confinement property is closely related to the Debye mass generation effect which is absent in the pure dipole plasma [13]. As a consequence, the confinement of electrically charged particles disappears. The system experiences a confinement-deconfinement phase transition due to the monopole binding mechanism.

One can use these heuristic arguments to estimate the phase transition temperature. In continuum theory this analy-

sis was made in Ref. [8] where compact electrodynamics was represented as a limit of the Georgi-Glashow model. The phase transition in this theory occurs at a temperature $T=g_3^2/(2\pi)$. This result was obtained under the condition that the average size of the effective magnetic dipole is not an infrared divergent quantity, as is the case in the confinement phase.

However, in lattice gauge theory the considered quantities are all finite and the considerations should be modified compared to the continuum case. The difference between monopole and dipole plasmas can only be seen if the mean distance $\overline{r}$ between the constituent monopoles becomes comparable to the dipole size $\overline{d}$. The distance $\overline{r}$ can be expressed, via the density of the monopoles ρ, as $\overline{r}=\rho^{-1/3}$. Thus the phase transition happens when the dipole size and the average distance between monopoles become of the same order,

$$\overline{d}=\xi\,\rho^{-1/3}, \tag{2.3}$$

where ξ is a geometrical factor of order unity. For both quantities $\overline{d}$ and ρ, estimates can be easily obtained on the lattice, while the factor ξ is to be defined from a simulation.

We consider a 3D compact $U(1)$ gauge model on the $L_s^2\times L_t$ lattice with the action written in the Villain representation,

$$\mathcal{Z}=\int_{-\pi}^{+\pi}\mathcal{D}\theta\sum_{n(c_2)\in\mathbb{Z}}\exp\left\{-\frac{\beta_V}{2}\|\mathrm{d}\theta+2\pi n\|^2\right\}, \tag{2.4}$$

where θ is the compact $U(1)$ gauge field and n is the integer-valued auxiliary tensor field variable. β_V is the Villain coupling constant.

To relate this to the numerical simulations, we also consider a formulation of the compact $U(1)$ gauge theory with Wilson action:

$$S=\beta\sum_P\,[1-\cos\theta_P]. \tag{2.5}$$

The Villain coupling constant β_V is related to the Wilson coupling β as [14]

$$\beta_V(\beta)=\left[2\log\left(\frac{I_0(\beta)}{I_1(\beta)}\right)\right]^{-1}, \tag{2.6}$$

where $I_{0,1}$ are the standard modified Bessel functions.

The partition function [Eq. (2.4)] can be rewritten in the following *grand canonical* form, i.e., represented as a sum over monopole charges in the (dual) lattice cubes [14]:

$$\mathcal{Z}\propto\mathcal{Z}_{mon}=\sum_{m(c_3)\in\mathbb{Z}}\exp\{-2\pi^2\beta_V(m,\Delta^{-1}m)\}. \tag{2.7}$$

Here Δ^{-1} is the inverse of the Laplacian operator on an asymmetric lattice and m_c denotes the monopole charge in the cube c_3. The inverse Laplacian for lattice sizes L_s and L_t is given as

$$\Delta^{-1}(\vec{x};L_s,L_t)=\frac{1}{2L_s^2L_t}\sum_{\vec{p}^2\neq 0}\frac{e^{i(\vec{p},\vec{x})}}{3-\sum_{i=1}^{3}\cos p_i}, \tag{2.8}$$

where $p_{1,2}=0,\ldots,2\pi(L_s-1)/L_s$ and $p_3=0,\ldots,2\pi(L_t-1)/L_t$.

In order to estimate the average distance between the monopole and antimonopole constituents in a dipole state (i.e., the dipole size) we use the *canonical* monopole-antimonopole (dipole) partition function, which can be easily read from Eq. (2.7):

$$\mathcal{Z}_{dip}^{(2)}=\mathrm{const}\cdot\sum_{\substack{x\\ x^2\neq 0}}\exp\{4\pi^2\beta_V[\Delta^{-1}(x;L_s,L_t)-\Delta^{-1}(0;L_s,L_t)]\}, \tag{2.9}$$

the sum extends over all lattice separations x between the monopole and antimonopole. The zero distance between these objects is excluded (since this case does not correspond to a dipole state). The rms dipole size $\overline{d}$ is given by

$$\overline{d^2}(\beta_V;L_s,L_t)=\frac{1}{\mathcal{Z}_{dip}^{(2)}}\sum_x\,x^2\exp\{4\pi^2\beta_V[\Delta^{-1}(x;L_s,L_t)-\Delta^{-1}(0;L_s,L_t)]\}, \tag{2.10}$$

where the actual distance squared, x^2, is evaluated by taking into account the periodic boundary conditions of the lattice. The sums cannot be taken analytically.

The monopole density ρ can be read off from Eq. (2.7),

$$\rho(\beta;L_s,L_t)=2\exp\{-2\pi^2\beta_V(\beta)\Delta^{-1}(0;L_s,L_t)\}, \tag{2.11}$$

where the dependence on the lattice geometry is indicated explicitly. Note that in this formula no interaction between monopoles is taken into account, and we refer to it as ''bindingless.'' Only the local self-interaction of monopoles is accounted for via the Coulomb propagator $\Delta^{-1}(0)$ in the fugacity. We discuss the binding effects on the monopole density in Sec. V.

The geometrical factor ξ is to be defined from the numerical data. To this end we assume that this factor is a constant quantity which does not depend on the lattice extensions. Indeed, it gives an estimate how large the intradipole distances should be compared to the monopole density in order for the dipole field to be screened. This is quite a strong assumption which, however, turns out to be reasonable, as will we see below. To define the factor ξ we substitute Eqs. (2.10) and (2.11) into Eq. (2.3), and use numerical values for β_c presented in Ref. [7]. For the lattices $16^2\times L_t$, $L_t=4,6$, and 8 we obtain $\xi=0.723(58)$, $0.622(47)$, and $0.646(116)$, respectively. These numbers coincide with each other within numerical errors. Taking the average over L_t we obtain $\overline{\xi}\approx 2/3$. In what follows we take

$$\xi=2/3, \tag{2.12}$$

TABLE I. The critical coupling constant β_c^{th} calculated using Eqs. (2.6), (2.3), (2.10), (2.11), and (2.12) for different lattices $L_s^2 \times L_t$ compared to lattice Monte Carlo results of Ref. [7]. Note that our results for the lattice $32^2 \times 8$ are slightly higher than that of Ref. [7]; see the text.

	$L_s=16$		$L_s=32$		$L_s=64$
L_t	β_c^{th}	β_c	β_c^{th}	β_c	β_c^{th}
4	1.87	1.83(2)	2.01	–	2.10
6	2.04	2.08(2)	2.26	2.18(3)	2.44
8	2.12	2.14(5)	2.39	2.30(2)	2.62

and then solve Eqs. (2.3), (2.11), and (2.10) with respect to the Villain coupling β_V. Then we finally estimate the critical Wilson coupling $\beta_c^{\rm th}$ with the help of Eq. (2.6). The results for lattices of various sizes are represented in Table I, and compared with pseudocritical couplings β_c obtained in lattice simulations of Ref. [7]. The agreement between the data and our estimates is within 4%. Thus the simple heuristic arguments based on the monopole-dipole picture work surprisingly well.

III. PHASE TRANSITION AND CONFINEMENT

We have performed our numerical study of $(2+1)$D compact electrodynamics using the Wilson action [Eq. (2.5)]. The lattice coupling β is related to the lattice spacing a and the continuum coupling constant g_3 of the 3D theory as follows:

$$\beta = \frac{1}{a\, g_3^2}. \tag{3.1}$$

Note that in three-dimensional gauge theory the coupling constant g_3 has a dimension mass (to the power of 1/2).

The lattice corresponding to the finite temperature is asymmetric: $L_s^2 \times L_t$, $L_t < L_s$. In the limit $L_s \to \infty$ the temporal extension of the lattice L_t is related to the physical temperature $L_t = 1/(Ta)$. Using Eq. (3.1) the temperature is given via the lattice parameters as follows:

$$\frac{T}{g_3^2} = \frac{\beta}{L_t}. \tag{3.2}$$

Thus, at a fixed lattice size lower (higher) values of the lattice coupling constant β correspond to lower (higher) temperatures.

Our simulations have been performed mainly on a $32^2 \times 8$ lattice. In the present paper we do not intend to study finite size scaling aspects of this model. The local Monte Carlo algorithm is based on a five-hit Metropolis update sweep followed by a microcanonical sweep. For better ergodicity, in particular in the presence of an external field (considered in a companion paper), global updates are also included. Following the ideas of Ref. [15], the global refreshment step consists of an attempt to add an additional unit of flux with a randomly chosen sign in a direction randomly selected among the three, to the dynamical gauge field subject to a global Metropolis acceptance check.

For example, one unit of flux in ij plane is introduced with the help of the following gauge field shift [15] $\theta_i \to [\theta_i + \tilde{\theta}_i]_{\rm mod 2\pi}$:

$$\tilde{\theta}_j = \frac{\pi}{L_i}(2x_i - L_i - 1), \quad \tilde{\theta}_j = 0 \quad \text{for} \quad x_j \neq L_j,$$

$$\tilde{\theta}_i = \frac{2\pi}{L_i L_j}(1 - x_j), \quad \tilde{\theta}_k = 0, \quad k \neq i,j.$$

The acceptance rate of the global step changes within the considered β range from roughly 0.7 (confinement phase) to 0.2 (deconfinement phase). One total Monte Carlo update cycle consists of two combined local Metropolis and microcanonical sweeps (requiring an acceptance rate of 0.5 for the Metropolis step) and the global update described above.

In order to localize the deconfinement transition, it is convenient to study the expectation values of the two bulk operators,

$$\langle |L| \rangle = \frac{1}{L_s^2}\left\langle \left| \sum_{\mathbf{x}} L(\mathbf{x}) \right| \right\rangle, \quad \langle |L|^2 \rangle = \frac{1}{L_s^2}\left\langle \left| \sum_{\mathbf{x}} L(\mathbf{x}) \right|^2 \right\rangle, \tag{3.3}$$

constructed from the Polyakov loop:

$$L(\mathbf{x}) = \exp\left\{ i \sum_{z=1}^{L_t} \theta_3(\mathbf{x},\mathbf{z}) \right\}. \tag{3.4}$$

Here $\mathbf{x}=(x,y)$ is a two-dimensional vector. In the deconfinement phase the quantity $|L|$ is of the order of unity, while in the confinement phase it is close to zero in a finite volume, and vanishes in the infinite volume limit.

The behavior of the expectation value of the Polyakov loop vs the lattice coupling β is shown in Fig. 1(a). The low temperature phase $\beta < \beta_c$ corresponds to the confinement phase, while the high temperature phase is deconfining.

The susceptibility of the Polyakov loop,

$$\chi_L = \langle |L|^2 \rangle - \langle |L| \rangle^2, \tag{3.5}$$

is shown in Fig. 1(b). The peak of the Polyakov loop susceptibility corresponds to the pseudocritical β_c of the deconfinement phase transition. We have fitted the susceptibility near its maximum by the function

$$\chi_L^{\rm fit}(\beta) = \frac{c_1^2}{c_2^2 + (\beta - \beta_c)^2}, \tag{3.6}$$

where the critical coupling was estimated to be $\beta_c = 2.346(2)$ which is quite close to the result of Ref. [7]. The best fit is shown in Fig. 1(b) by a solid line.

To calculate the string tension we use an analog of plane-plane correlators of two Polyakov loops. In addition, averages of temporal Wilson loops have also been studied. More

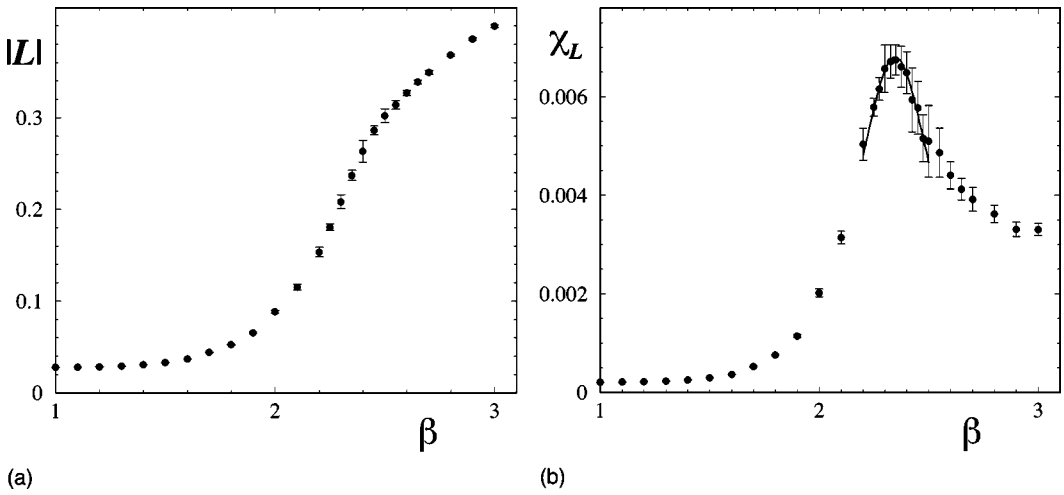

FIG. 1. (a) The expectation value of the absolute value of the average Polyakov loop [Eq. (3.3)] and (b) its susceptibility [Eq. (3.5)] vs β.

precisely, in $(2+1)$D systems, we define first sums of the Polyakov loops along a line parallel to a spatial lattice axis (e.g., in the y direction):

$$L_{\text{plane}}(x)=\sum_{y=1}^{L_s} L(x,y). \tag{3.7}$$

The plane-plane correlator may be written as a sum of point-point correlation functions:

$$\langle L_{\text{plane}}(0)L^*_{\text{plane}}(x)\rangle=\sum_{y_{1,2}=1}^{L_s}\langle L(0,y_1)L^*(x,y_2)\rangle. \tag{3.8}$$

The form of this correlator is expected to be

$$\langle L_{\text{plane}}(0)L^*_{\text{plane}}(x)\rangle=\text{const}\cosh\left[\sigma L_t\left(x-\frac{L_s}{2}\right)\right], \tag{3.9}$$

where σ is the temporal string tension. In Fig. 2(a) we show the fit of the Polyakov plane-plane correlator [Eq. (3.8)] by this fitting function in the confinement ($\beta=1.8$) and deconfinement ($\beta=2.5$) phases, respectively.

In Fig. 2(b) we present the fitted string tensions as functions of β. Above β_c the string tension quickly drops, but remains nonzero due to finite volume effects. The temporal string tensions obtained using either the Polyakov loop plane-plane correlators or the temporal Wilson loop averages roughly coincide with each other. The dashed curve represents the theoretical prediction for the string tension [14,16]:

$$\sigma(\beta)=\frac{4\sqrt{2}}{\pi\sqrt{\beta_V(\beta)}}\exp\{-\pi^2\beta_V(\beta)\Delta^{-1}(0;L_s,L_t)\}. \tag{3.10}$$

Agreement between the prediction and the numerical results is reached only in the vicinity of the phase transition point, $\beta\approx 2.3$. In order to understand these differences, we now turn to a closer investigation of the monopole properties.

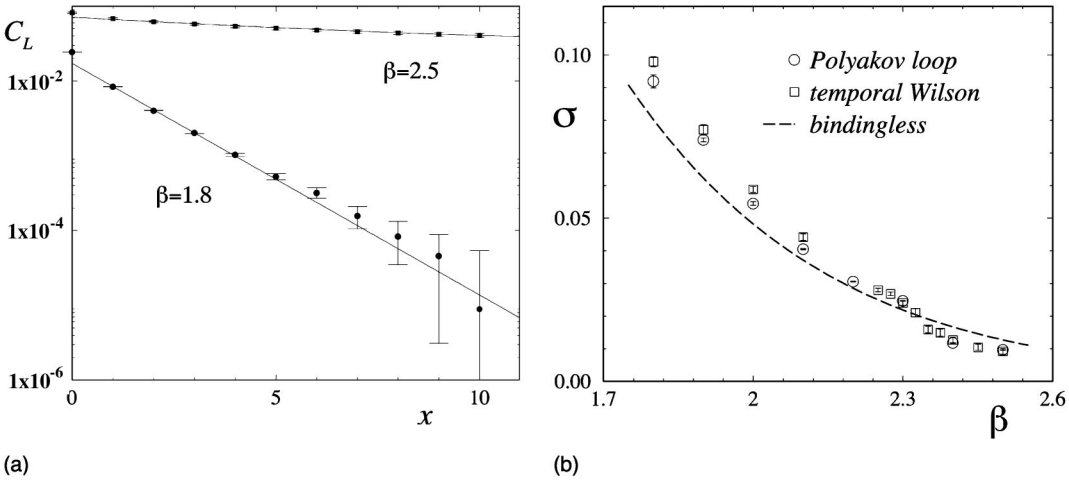

FIG. 2. (a) Fit of the Polyakov plane-plane correlator [Eq. (3.8)] using Eq. (3.9) in the confinement ($\beta=1.8$), and deconfinement ($\beta=2.5$) phases. (b) String tensions as functions of β compared with the bindingless theoretical result [Eq. (3.10)].

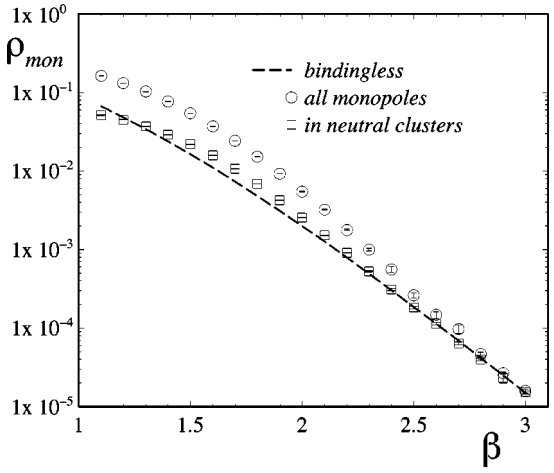

FIG. 3. The density of all monopoles and of monopoles in neutral clusters vs β.

IV. PROPERTIES OF THE MONOPOLE-ANTIMONOPOLE SYSTEM

The basic quantity describing the behavior of the monopoles is the monopole density $\rho=\Sigma_c|m_c|/(L_s^2L_t)$, where m_c is the integer valued monopole charge inside the cube c defined in the standard way [17],

$$m_c=\frac{1}{2\pi}\sum_{P\in\partial c}(-1)^P[\theta_P]_{\mathrm{mod}\,2\pi}, \tag{4.1}$$

where the plaquette orientations relative to the boundary of the cube are taken into account. The density of the total number of monopoles is a decreasing function of the lattice coupling β (or the temperature), as shown in Fig. 3 by circles. At high temperatures (large β) the monopoles are dilute and form dipole bound states. Typical monopole configurations in both phases are visualized in Fig. 4.

In Fig. 3, with the dashed line we show the density of the monopoles calculated using Eq. (2.11) for comparison. As in the case of the string tension, the predicted monopole density is in agreement with the numerical data only near β_c.

Equation (2.11) is based on a single monopole contribution to the partition function; thus it does not take the pairing of the monopoles into account. The effect of constituent monopole pairing (dipole formation) due to finite temperature can explain the deviations from the bindingless case seen in this Fig. 3. In the confinement phase the density of the monopoles is larger than the prediction of Eq. (2.11). Indeed, we expect that the formation of the bound state decreases the total energy (action) of the chosen monopole and antimonopole. As a result binding favors the creation of additional monopoles by quantum fluctuations. This tendency increases with larger β; however the cost of creating new monopoles also grows.

Note that the entropy of the bound state is smaller than the entropy of a free monopole and an antimonopole. However the entropy effect does not seem to change essentially near the phase transition.

We remind the reader that on the classical level dipoles are formed both in the confinement and deconfinement phases due to the logarithmic potential between the monopoles. However, at low temperatures the dipole size is larger than the average distance between the monopoles; therefore, the dipole formation does not destroy confinement.

One can analyze the monopole pairing, studying the cluster structure of the monopole ensemble extracted from the Monte Carlo configurations. For our purposes, clusters are defined as follows: clusters are connected groups of monopoles and antimonopoles, where each object is separated from at least one neighbor belonging to the same cluster by a distance less than or equal to $R_{\max}$. In the following we use $R_{\max}^2=3\ a^2$ which means that neighboring monopole cubes should share at least one single corner.[1] Note that the increase of the coupling constant leads not only to an increase

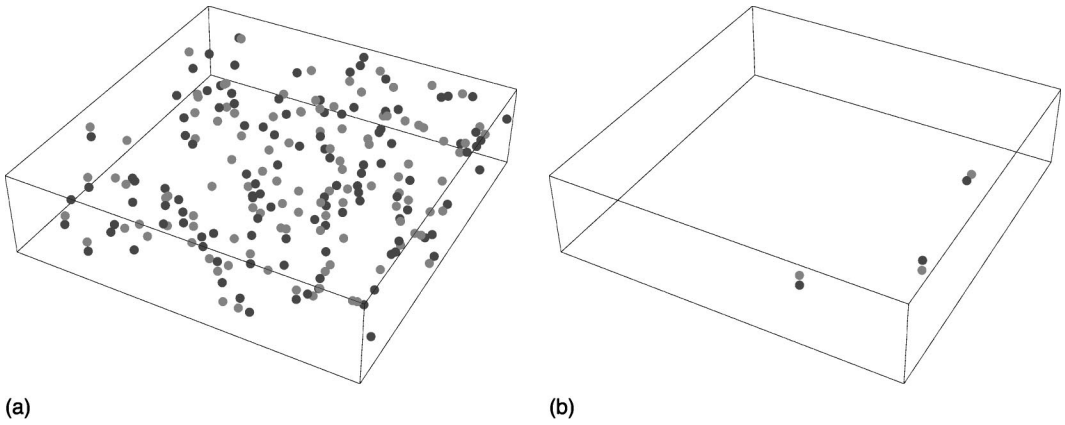

FIG. 4. Typical monopole configurations for (a) the confinement phase ($\beta=1.6$) and (b) the deconfinement phase ($\beta=2.5$).

[1]In Ref. [18] a similar definition was used to investigate tightly packed clusters with $R_{max}=a$. In our case the condition for the cluster is more relaxed.

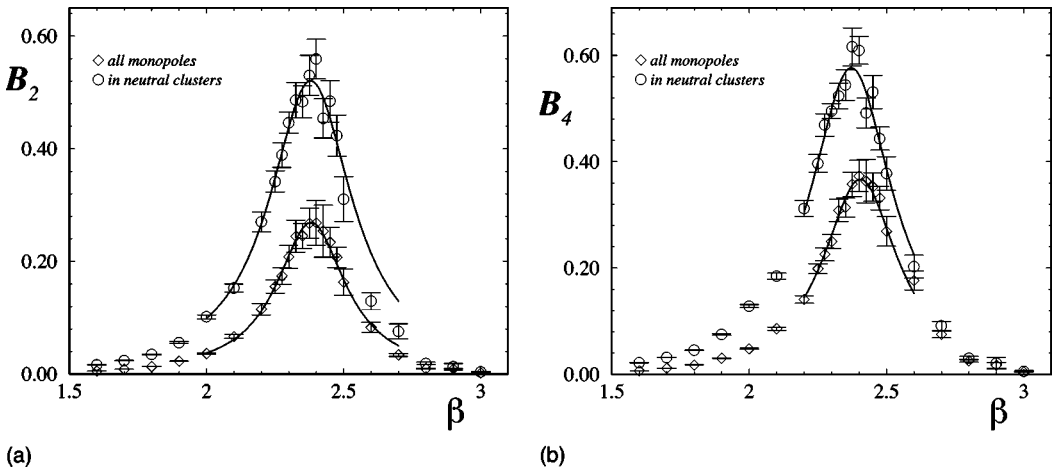

FIG. 5. The second (a) and the fourth Binder (b) cumulants according to Eq. (4.3) for the total (anti)monopole density and the corresponding densities enclosed in neutral clusters. The fits are shown as solid lines.

of the temperature [Eq. (3.2)], but to a decrease of the lattice spacing a as well [Eq. (3.1)]. Thus at different β the same characteristic distance $R_{\max}$ corresponds to different physical scales. Therefore our results below are of only a qualitative nature.

A monopole cluster is neutral if the charges of the constituent monopoles sum up to zero. In Fig. 3, with squares we show the density of monopoles belonging to neutral clusters as a function of β. The difference between this density and the total monopole density amounts to a factor 3 at $\beta \approx 1$ and becomes smaller at larger β. At large β (entering the deconfinement phase) approximately every second monopole or antimonopole belongs to a neutral cluster. At still larger β's almost all monopoles are in neutral clusters.

We are confident that the fluctuation of monopole numbers signals a deconfining phase transition. This is demonstrated by studying the second and (modified) fourth Binder cumulants of the total number of monopoles and antimonopoles [and of the number of anti monopoles being part of neutral clusters]. In Fig. 5 we present the cumulants, with M denoting the respective number:

$$B_2 = \frac{\langle M^2 \rangle}{\langle M \rangle^2} - 1, \tag{4.2}$$

$$B_4 = \frac{\langle M^4 \rangle}{3\langle M^2 \rangle^2} - \frac{1}{3}. \tag{4.3}$$

Similarly to the Polyakov loop susceptibility these quantities are suitable to localize the deconfining phase transition. We fit these cumulants by

$$B_n^{\rm fit}(\beta) = \frac{c_1^2}{c_2^2 + (\beta - \beta_c)^2}, \quad n = 2,4. \tag{4.4}$$

The fits are shown by solid lines in Fig. 5, and the results for the pseudocritical couplings β_c are given in Table II.

Some details on the cluster structure at various values of β can be seen in Fig. 6(a). We show the fraction of monopoles and antimonopoles that are parts of clusters of size N. The cluster size is the number of monopoles and antimonopoles which belong to the given cluster. There is no separation according to the cluster's charge. In the confinement phase, $\beta = 1.5$, the fraction of monopoles slowly decreases with the cluster size N. The percentage of isolated (anti-) monopoles ($N = 1$ clusters) amounts to roughly 45% while clusters (with a size up to $N = 10$) contain the rest.

At the phase transition point ($\beta \approx 2.3$) the number of (anti)monopoles enclosed in larger clusters drops drastically. The monopole vacuum is composed mostly of individual (anti)monopoles (60%) and dipoles (40%). This observation can be reconciled with our theoretical expectation that all monopoles must become paired only if we accept that the unpaired monopoles are actually part of dipoles of sizes larger than $R_{\max}$. Deeper in the deconfined phase, however, at $\beta = 2.8$ practically 90% of the (anti)monopoles form tightly bound states with sizes smaller than $R_{\max} = \sqrt{3}\ a$.

As we discussed above, we expect that the force in the spatial direction is larger than the force along the temporal direction z. This fact can be qualitatively analyzed with the help of the cluster sphericity

$$R_{\rm size}(N) = \frac{\langle |\Delta z| \rangle_N}{\sqrt{\langle \Delta x| \rangle_N^2 + \langle |\Delta y| \rangle_N^2}}, \tag{4.5}$$

where $\langle |\Delta x| \rangle_N$ is the average distance from the center of the cluster in the x direction, etc., for a cluster size N. If the clusters are elongated predominantly in the temporal direction this quantity would be larger than unity, and smaller otherwise. In Fig. 6(b) we show the dependence of the sphericity $R_{\rm size}$ on the cluster size N for various β values. Small

TABLE II. Pseudocritical couplings β_c from the fits to the Binder cumulants [Eqs. (4.2) and (4.3)].

Cumulant	Second	Fourth
total	2.380(3)	2.404(4)
neutral	2.379(5)	2.372(3)

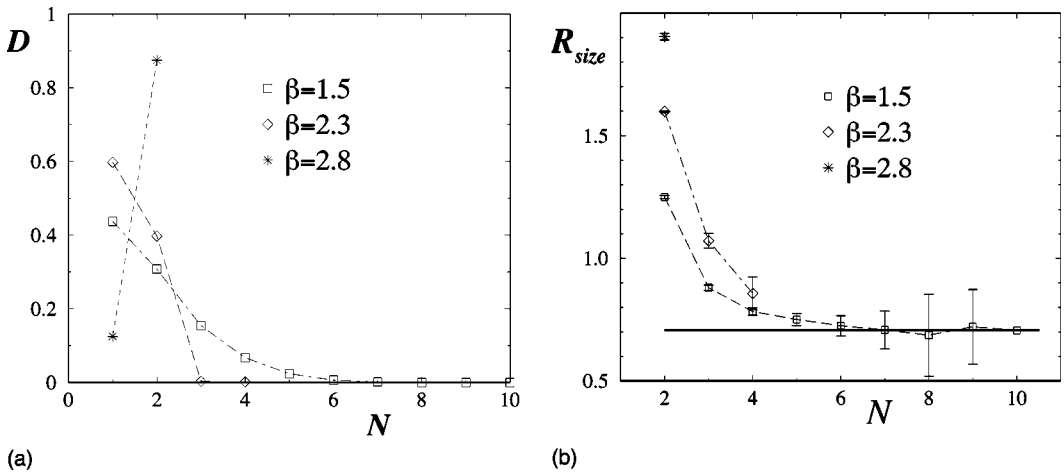

FIG. 6. (a) The cluster structure at various of the coupling constant β. The cluster distribution is shown as a function of the number of constituent monopoles inside clusters, N. (b) The cluster shape function [Eq. (4.5)], for various β.

clusters are directed predominantly along the temporal direction, as expected, at all β. With larger β the elongation becomes stronger. For large clusters the direction of the cluster is random, since in this case the cluster shape function is very close to $1/\sqrt{2}$ [this follows directly from definition (4.5)]. This random limit is marked by the solid line in Fig. 6.

V. CONFINEMENT AND MONOPOLES

We have observed that agreement between predictions from a theory without monopole binding and our results from finite temperature simulation results is reached only in the vicinity of the phase transition point, $\beta \approx 2.3$. In the confinement phase both the measured temporal string tension and monopole density are larger compared to the bindingless predictions, see Figs. 2(b) and 3.

As we have discussed, due to monopole binding the density of the monopoles is increased compared to the noninteracting case. However, the size of the dipoles in the confinement phase is larger than the average distance between the ordinary monopoles calculated from their total density. Therefore, monopoles bound in dipoles due to classical logarithmic potential still give a contribution to the string tension.

It is interesting to check how the monopole density fits into the theoretical predictions of the string tension [Eq. (3.10)]. Using this predicted relation, in Fig. 7 we compare the ratio R_σ between the measured string tension σ (from plane-plane correlators of Polyakov loops) with a calculated ''theoretical'' string tension $\sigma^{\rm th}$ using as input the *measured* monopole density ρ:

$$R_\sigma = \frac{\sigma}{\sigma^{\rm th}}. \tag{5.1}$$

Here $\sigma^{\rm th}$ is given in accordance with Eqs. (2.11) and (3.10) via

$$\sigma^{\rm th} = \frac{4}{\pi}\sqrt{\frac{\rho(\beta)}{\beta_V(\beta)}}, \tag{5.2}$$

and β_V is defined in Eq. (2.6).

The circles shown take into account all active monopoles, i.e., isolated ones and those from charged monopole clusters which might be thought to be responsible for the string tension. The ratio is close to unity, indicating the fact that the charged monopoles provide the major contribution to the string tension, as expected. Note that in the deconfinement phase the string tension is nonzero due to the finite-size effects discussed below. The squares in Fig. 7(a) are related to ratio (5.1) in which all monopoles are taken into account. In both phases this ratio is smaller than unity: a neutral fraction of the monopoles bound in the small dipole pairs does not contribute to the string tension.

The small value of the string tension remaining after passing the deconfinement transition at this finite lattice can be explained from the point of view of the dipole picture as follows. Test particles separated by distances smaller than sizes of certain dipoles are influenced by the constituent

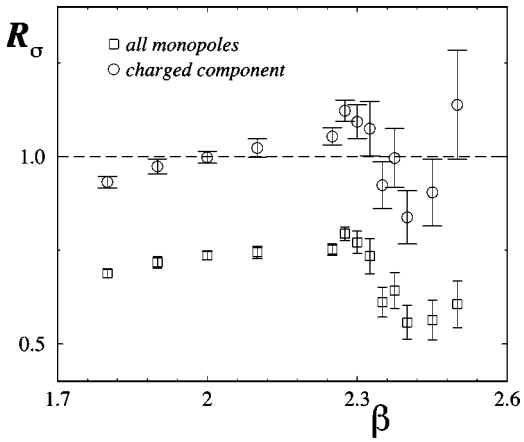

FIG. 7. The ratio of the temporal string tensions [Eq. (5.1)] vs β.

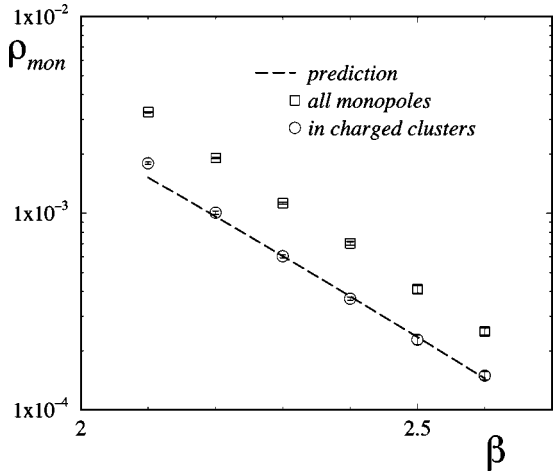

FIG. 8. The density of all monopoles and of monopoles in charged clusters vs β for a 32^3 lattice compared to prediction (2.11).

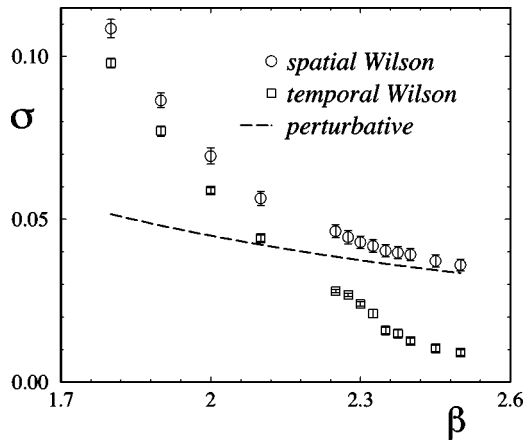

FIG. 9. The spatial string tension vs β.

monopoles of those dipoles. The monopoles make contributions to the string tension term. On the finite lattice the maximal distance between the test particles is of the order of the lattice size. Therefore, dipoles of the same size could be responsible for the nonvanishing small string tension. Dipoles of these sizes may be present in the deconfinement phase (with a probability that decreases with an increase of the lattice size). However, this does not contradict the criterion used to locate the phase transition in the previous sections, since dipoles of such large sizes are heavily suppressed.

Dipole formation due to Coulomb forces also occurs at zero temperature. This effect increases the monopole density compared to that in the ''bindingless'' world. To check this, in Fig. 8 we compare the total density of monopoles and the exclusive density of monopoles residing in charged clusters (the latter includes free monopoles and antimonopoles) for a 32^3 lattice. The charged monopoles comprise around 55% of the total monopole density. This ratio does not depend on the value of the coupling constant β, indicating that the scaling behaviors of charged and neutral clusters are the same. The charged fraction of the monopoles is perfectly described by the ''bindingless'' formula [Eq. (2.11)] for the monopole density. This formula is incorporated implicitly into the theoretical prediction of the string tension [Eq. (3.10)], which works well according to Ref. [19]. Thus only monopoles from charged clusters (including separate monopoles) contribute to the string tension, while the binding effect causes the appearance of a large fraction of inactive neutral clusters.

Finally, we have measured the spatial string tension: the coefficient in front of the area term in the spatial Wilson loops. This string tension σ_s has been obtained by means of the standard diagonal Creutz ratios. The results are presented in Fig. 9 as functions of β. As expected, the spatial string tension does not vanish and behaves smoothly across the deconfining phase transition. In contrast, in this figure we also show the ''true,'' i.e., temporal string tension extracted from temporal Wilson loops, which drops down to the level of the finite-volume correction that we have just discussed.

At sufficiently high temperatures the system might be treated as two-dimensional with an effective 2D coupling constant $\beta^{(2D)}=L_t\beta$. Moreover, since the monopole density is low at large β (in deconfinement), the model becomes effectively noncompact. Thus the spatial Wilson loop behavior in this regime is given by the perturbative one-photon exchange. In two dimensions the Coulomb law provides the linearly confining potential $V^{(2D)}(R)=R/2$, corresponding to the spatial string tension

$$\sigma_s^{\rm th}(\beta)=\frac{1}{2\beta^{(2D)}}=\frac{1}{2L_t\beta}, \tag{5.3}$$

which is shown in Fig. 9 by the dashed line. The spatial string tension data and the curve approach each other for sufficiently large β. However, in the confinement phase the monopoles make a significant contribution to the spatial string tension.

VI. SUMMARY

In this paper we have considered a mechanism for a finite temperature deconfinement phase transition in three dimensional compact electrodynamics based on monopole binding. The considerations are similar to those given in Ref. [8] for the continuum theory, and they incorporate features of the lattice geometry. This allows us to predict the pseudocritical coupling as a function of the lattice size.

In our numerical simulations we have demonstrated that the monopoles are sensitive to the phase transition despite the fact that the monopole density itself behaves smoothly across the transition. The pseudocritical couplings found by the Binder cumulants of the density are very close to that identified using the Polyakov loop susceptibility. We stress that we did not intend to study the finite size scaling behavior of this model.

Based on the observation used to find β_c in this way, we have studied the monopole properties in more detail. We have found that both the monopole density and the string tension differ from the predictions based on a model which does not take the monopole binding effects into account.

However we found numerically that the ratio between these two quantities derived in that model [given by Eq. (3.10)] remains valid in the confinement phase.

We have observed that dipole formation occurs both in confinement and deconfinement phases. In the deconfinement phase tightly bound dipoles—which are safely identified by a cluster algorithm—dominate in the vacuum. The dipoles are oriented dominantly in the temporal direction. These features are in agreement with general expectations discussed in Secs. I and II.

At the confinement phase transition we observe mostly clusters with two constituents or single monopoles and antimonopoles. Further decreasing the temperature (or β), the monopoles become dense and form connected clusters (on a coarser and coarser lattice) inclosing various numbers of monopoles and antimonopoles. The largest clusters are more and more spherical. Whether the observed properties of the dipole gas formation survives in the continuum limit deserves an additional study.

When the phase transition is mediated by charged objects, one could expect that external fields will influence the phase transition. In our case the natural question arises of what will happen to the confinement-deconfinement phase transition. For non-Abelian theories in $3+1$ dimensions it was recently concluded, from a study of the expectation value of the Polyakov loop [20], that confinement seems to become restored under the influence of an external chromomagnetic field. In an accompanying paper [21] we will report on a study of our model under such external conditions, concerning the influence of confinement and relevant properties of the monopole system.

ACKNOWLEDGMENTS

The authors are grateful to P. van Baal, M. I. Polikarpov, and J. Zaanen for interesting discussions. M.N.Ch. acknowledges a support of Sächsisches Staatsministerium für Kunst und Wissenschaft, Grant No. 4-7531.50-04-0361-01/16 and kind hospitality of NTZ and the Institute of Theoretical Physics of Leipzig University. The work of M.N.Ch. was partially supported by Grants Nos. RFBR 99-01230a, RFBR 01-02-17456, and CRDF Award No. RP1-2103. E.-M.I. acknowledges the support by the Graduiertenkolleg ''Quantenfeldtheorie'' for a working visit to Leipzig.

[1] A.M. Polyakov, Nucl. Phys. **B120**, 429 (1977).
[2] M. Göpfert and G. Mack, Commun. Math. Phys. **82**, 545 (1981).
[3] T. Sterling and J. Greensite, Nucl. Phys. **B220**, 327 (1983).
[4] N. Parga, Phys. Lett. **107B**, 442 (1981).
[5] B. Svetitsky, Phys. Rep. **132**, 1 (1986).
[6] J.M. Kosterlitz and D.J. Thouless, J. Phys. C **6**, 1181 (1973).
[7] P.D. Coddington, A.J. Hey, A.A. Middleton, and J.S. Townsend, Phys. Lett. B **175**, 64 (1986).
[8] N.O. Agasyan and K. Zarembo, Phys. Rev. D **57**, 2475 (1998).
[9] G. Dunne, I.I. Kogan, A. Kovner, and B. Tekin, J. High Energy Phys. **01**, 032 (2001).
[10] T. Schäfer, E.V. Shuryak, and J.J.M. Verbaarschot, Phys. Rev. D **51**, 1267 (1995); R. Rapp, T. Schäfer, E.V. Shuryak, and M. Velkovsky, Ann. Phys. (N.Y.) **280**, 35 (2000); E.-M. Ilgenfritz and E.V. Shuryak, Phys. Lett. B **325**, 263 (1994).
[11] M.N. Chernodub, F.V. Gubarev, and E.-M. Ilgenfritz, Phys. Lett. B **424**, 106 (1998); M.N. Chernodub, F.V. Gubarev, E.-M. Ilgenfritz, and A. Schiller, *ibid.* **443**, 244 (1998); **434**, 83 (1998).
[12] M.N. Chernodub, Phys. Rev. D **63**, 025003 (2001); hep-th/0011124; B.L. Bakker, M.N. Chernodub, and A.I. Veselov, Phys. Lett. B **502**, 338 (2001); I.I. Kogan, A. Kovner, and B. Tekin, J. High Energy Phys. **03**, 021 (2001).
[13] J. Glimm and A. Jaffe, Commun. Math. Phys. **56**, 195 (1977).
[14] T. Banks, R. Myerson, and J. Kogut, Nucl. Phys. **B129**, 493 (1977).
[15] P.H. Daamgaard and U.M. Heller, Nucl. Phys. **B309**, 625 (1988).
[16] J. Ambjorn, A.J. Hey, and S. Otto, Nucl. Phys. **B210**, 347 (1982).
[17] T.A. DeGrand and D. Toussaint, Phys. Rev. D **22**, 2478 (1980).
[18] Z. Schram and M. Teper, Phys. Rev. D **48**, 2881 (1993).
[19] R.J. Wensley and J.D. Stack, Phys. Rev. Lett. **63**, 1764 (1989).
[20] P. Cea and L. Cosmai, hep-lat/0101017.
[21] M.N. Chernodub, E.-M. Ilgenfritz, and A. Schiller (unpublished).